Frontiers in Heat and Mass Transfer (FHMT), 19, 39 (2022)
DOI: 10.5098/hmt.19.39

Global Digital Central
ISSN: 2151-8629

Frontiers in Heat and Mass Transfer

Available at www.ThermalFluidsCentral.org

HYDROTHERMAL CHARACTERISTICS OF WATER FLOW INTO A DIMPLED TUBE HEAT EXCHANGER: A PARAMETRIC STUDY

Mousa Aqeel Ali* Saad Najeeb Shehab

Department of Mechanical Engineering, College of Engineering, Mustansiriyah University, Baghdad, Iraq.

ABSTRACT

In this study, the hydrothermal water flow characteristics using a dimpled inner tube heat exchanger are investigated experimentally and numerically. A numerical analysis has performed on two types of dimpled tubes (In-lined and staggered distributions) for two distribution angles 60º and 90º, and two dimple diameters (4 mm and 6 mm) with constant pitch ratio (X/d=8). In experimental part, a staggered arrangement dimpled inner tube distribution with angle 60º, dimple diameter of 6 mm and constant pitch ratio (X/d=8)is used as well as plain tube. The results illustrate that the heat transfer as Nusselt number for case of staggered dimpled inner tube improved between 7.55 and 11.2 times than plain tube. The numerical results demonstrate that staggered distribution of dimpled inner tube improve the Nusselt number nearly with 50% bigger than that the in-line distribution dimpled tube. The thermal performance factor (TPF) varied from 1.67 to 5.22 for tubes with in-line arrangement while from 4.91 to 8.633 for dimple tubes with a staggered arrangement.

Keywords: *Parametric study, dimple tube, in-line arrangement, staggered arrangement, hydrothermal Characteristics*

1. INTRODUCTION

Industrial activities that consume a large proportion of energy resources have captivated the consideration of many researchers. As a result, enhancing thermal efficiency has emerged as one of the most pressing issues (Promvonge 2008; Bergles 2002; Datt *et al.* 2019; Ali *et al.* 2022). Traditional heat exchangers with smooth tubes have a low and inefficient thermal performance, making them unsuitable for reducing energy use and increasing economic gains. Fins, twisting taps, ribs, and dimples are only some of the heat transfer enhancement methods that have been carefully examined over the past few decades. Many industrial applications of dimpled tube like, heat exchangers, cooling systems, solar collectors (Solanki and Kumar 2018; Xie *et al*. 2014).

Over the past decade, numerous researchers have studied dimpled tube for enhancing heat transfer rate. Fan and Yin (2008) studied the impact of different geometrical parameters of protrusions on heat transfer and pressure drop on an evaporator with a dimpled jacket. The usual k–e model was used to forecast turbulent flow. Protrusion spacing was found to have a significant impact on heat transmission. It has also been found that the staggered layout provides higher thermal-hydraulic performance than the in-line arrangement. Shafaee *et al*. (2016) conducted a series of experiments using the dimpled tube to study heat transfer performance. There was a noticeable difference in the heat transmission performance between the interior and exterior of the drop-down surface. Chen *et al.* (2001) examined the efficiency of dimpled tubes' heat transfer performance at various depths and dimples pitches. They found that when the Reynolds number remained constant, thermal efficiency increased from 1.25-2.37, but at constant flow rates, it increased from 1.15-1.84. Thianpong *et al.* (2009) carried out experiments work on the dimpled tubes with twisted tape at different Reynolds numbers by using water as a working fluid. The results demonstrated that heat transfer performance is significantly impacted by the pitch ratio and twist ratio. Wang *et al.* (2009) investigated different arrangements of dimpled (in-lined and staggered arrays). Hot water surrounded the tube's exterior, while cold air ran along the tube's inside. They observed that the staggered design offered more improvement than the aligned arrays. Wang *et al.* (2010) experimentally studied the dimpled with two shapes, the spherical dimpled tube, and the ellipsoidal dimpled tube. They observed that the ellipsoidal dimpled tube enhanced more effectively than the spherical dimpled tube. Kumar *et al.* (2016) experimented with the protruding tube, which worked well. According to the results, Protruded surface tubes significantly improved heat transfer and friction. Aroonrat *et al*. (2017) experimentally investigated condensation heat transfer and pressure drop characteristics of R-134a flowing inside horizontal smooth and dimpled tubes. It is noticed that a tube with dimples produces a higher heat transfer coefficient and frictional pressure drop than a tube with a smooth tube. Li *et al.* (2016) conducted experiments using a double tube heat exchanger and dimpled tubes. They discovered a heat transfer increase that was two hundred percent higher than that of a smooth tube. Liang *et al.* [14] studied the heat transfer mechanism for the elliptical protruded tube quantitatively. The discussion was held regarding the impact of protrusion configuration, depth, pitch, number, axis ratio, and angle on thermal-hydraulic performance. They reported that the protrusion volume significantly affects thermal-hydraulic performance. Liang *et al.* (2019) and Xie *et al.* (2018a) performed the extrusion of a conventional smooth tube to create ETDP-enhanced tubes with dimples and protrusions. As a result of superior flow mixing, interrupted boundary layers, periodic jet flows, and swirl flows created by dimples and protrusions, they found that the ETDP outperformed the smooth tube in terms of increased heat transfer rate. Xie *et al.* (2018b) performed a numerical analysis of the improved tube with cross ellipsoidal dimples. According to these researchers, the transverse and longitudinal dimples showed that heat transport was significantly improved. Xie *et al*. (2019) studied a new model of enhanced tubes with teardrop dimples ETTD compared with (spherical and elliptical dimples). They found that the teardrop dimples significantly increase the heat transfer compared with (spherical /elliptical)dimple tubes. Li *et al.* (2016) conducted simulation and

* *Corresponding author. Email: ehma026@uomustansiriyah.edu*

Global Digital Central
ISSN: 2151-8629

experimental studies on the improved tube with dimples. The results show that the dimples on the tube surface have a high heat transfer capacity. The staggered arrays' heat exchange properties outperformed the in-line dimples arrays on a technical level. Regarding total heat exchange performance, geometric parameters such as pitch, depth, dimple shape, and stars have a much more significant impact than the dimple diameter. Zheng *et al.* (2015) performed a numerical investigation of smooth tubes with discrete double inclined ribs. When the inclined ribs were examined, they were found to have the ability to create multiple vortices, with a PEC value ranging from 1.3 to 2.3. Vignesh *et al.* (2017) performed an experimental and numerical study of a water-based concentric tube heat exchanger with plain and spherical dimpled tubes operating at various mass flow rates. The results show that the dimples on the tube surface have the most acceptable heat transfer improvement. Jalghaf and Hatem (2017) looked at how a dimpled tube affected heat transfer coefficient and pressure drop in the tube for a Reynolds number range of (4000-16000) with air-fluid. There is an increase in heat transmission of 1.584 - 2 times when comparing the results of the Nusselt number comparison between the smooth tube and the present slot dimples tube.

The purpose of this research is to look at the effectiveness of employing a dimpled inner tube of heat exchanger on the thermal performance using two arrangements of dimpled tubes namely, in-line and staggered, two distribution angles 60º and 90º, and two dimple diameters of 4 mm and 6 mm for a wide range of Reynolds number from 5,000 to 20,000 as well as to find the best design of inner dimpled tube.

2. NUMERICAL PART

2.1 Model Geometry and Boundary Conditions

The design is the first step in any study. The formulation and innovation of a collection of ideas, as well as the selection of the finest solutions, are all part of the design. Following a thorough investigation, we arrived at the following dimensions: For the double pipe heat exchanger the pipe's outside internal diameter (72mm), external diameter (76mm), and length (L= 1200 mm) are made from stainless steel. for the inner pipe (dimples tube) made from copper with internal diameter (26.2 mm), external diameter (28 mm), and length (L= 1350 mm), two types of dimpled tubes (In-lined and staggered dimpled arrays) with two an angle of 60 and 90. Also, the effect of diameter of dimples (4, 6)mm have been discussed constant pitch of X/d=8, analysed and then compared performance with the smooth tube. The model geometry was design using SOLIDWORKS as seen in Figure 1. A set of boundary conditions were carefully defined to obtain meaningful solutions. Boundary conditions are described in each region on surfaces and are equivalent to experimental tests. These boundary conditions include: For inlet boundary conditions, the inlet water temperature of 60 C for hot water and 27 C for cold water. Four Reynolds number values of (5000, 10,000, 15,000, and 20,000), and the pressure at the outlet is zero. For outlet boundary condition the pressure of the water at the outlet of the tube is the same as the atmospheric pressure.

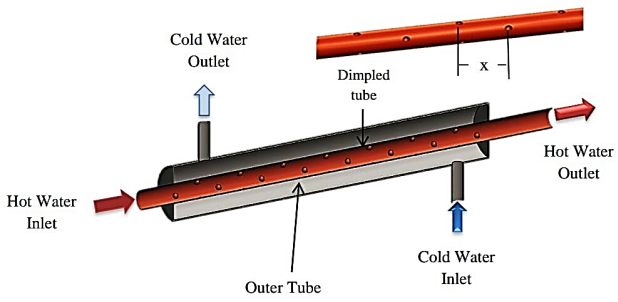

Fig. 1 Section view of the model geometry.

2.2 Numerical Solution

In ANSYS-Fluent software, mesh generation is one of the most essential phases of simulation. Mesh quality has a significant impact on the accuracy of the findings; if the mesh quality is high, the results will be accurate, whereas if the mesh quality is low, the results will be unsatisfactory. The Hexahedra mesh approach was utilized in this example, with the final mesh consisting of (2,489,956) elements, as seen in Figure 2.

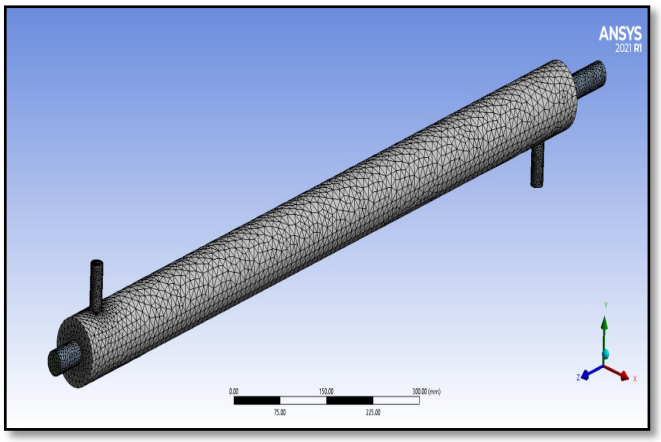

(a)

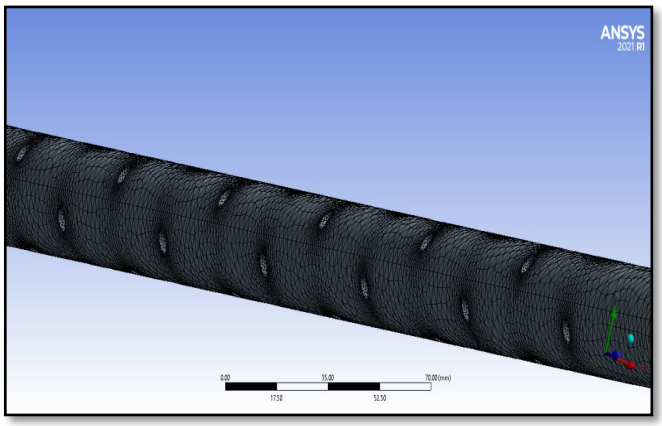

(b)

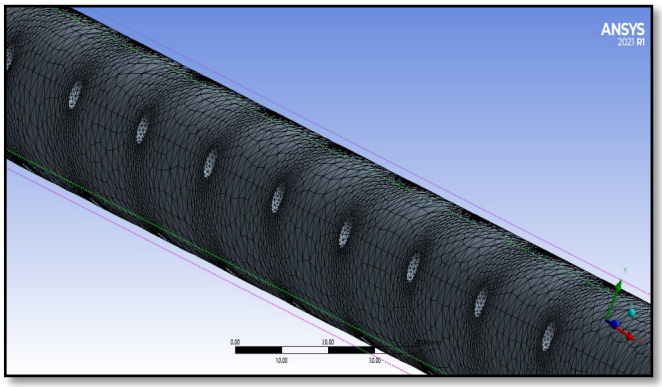

(c)

Fig. 2 Mesh generation (a) general models; (b) dimples tube with stagger arrangement; (c) dimples tube with in-line arrangement.

Global Digital Central
ISSN: 2151-8629

In order to find the hydrothermal properties of the water flow through a dimpled tube heat exchanger, the following assumptions have been used for the present study:
Steady-state condition, incompressible fully developed flow, turbulent flow, forced convection heat transfer, water properties are taken at bulk temperature, the material of the inner tube is homogeneous and isotropic, constant heat flux on the internal surface of the inner tube, the outer tube is assumed to be perfectly insulated finally, radiation heat transfer is negligible. Based on these assumptions, the fundamental governing equations of fluid dynamics—continuity, momentum, and energy—are the foundation of computational fluid dynamics. These are physics equations. Fluid mechanics is based on these three fundamental principles expressed mathematically in these three ways, and they serve as the foundation for all fluid dynamics (Bejan 2003; Davidson 2009):

- Continuity equation

$$\frac{\partial}{\partial x_i}(\rho u_i) = 0 \quad (1)$$

- Momentum equation

$$\frac{\partial}{\partial x_j}(\rho u_i u_j) = -\frac{\partial p}{\partial x_i} + \frac{\partial}{\partial x_j}(\mu + \mu_t)(\frac{\partial u_i}{\partial x_j} + \frac{\partial u_j}{\partial x_i}) \quad (2)$$

- Energy equation

$$\frac{\partial}{\partial x_i}(u_i T) = \frac{\partial}{\partial x_i}\left[\left(\frac{\mu}{Pr} + \frac{\mu_t}{Pr_t}\right)\frac{\partial T}{\partial x_i}\right] \quad (3)$$

Where ρ is fluid density, u is velocity, p is pressure, μ is dynamic viscosity, μ_t is turbulent viscosity, T temperature, Pr is the Prandtl number. The water fluid is the turbulent flow and incompressible fluid on the operating condition of fluid properties.

Equation for turbulence kinetic energy k equation and Specific dissipation rate ε:

$$\frac{\partial}{\partial x_j}(\rho k u_j) = \frac{\partial}{\partial x_j}\left[\left(\mu + \frac{\mu_t}{\sigma_k}\right)\frac{\partial k}{\partial x_j}\right] + \Gamma - \rho\varepsilon \quad (4)$$

$$\frac{\partial}{\partial x_j}(\rho \varepsilon u_j) = \frac{\partial}{\partial x_j}\left[\left(\mu + \frac{\mu_t}{\sigma_\varepsilon}\right)\frac{\partial \varepsilon}{\partial x_j}\right] + C_1\Gamma - C_2\frac{\varepsilon^2}{k+\sqrt{\nu\varepsilon}} \quad (5)$$

where Γ can be expressed as follows:

$$\Gamma = \overline{u_i u_j}\frac{\partial u_i}{\partial u_j} = \frac{\mu_t}{\rho}\left(\frac{\partial u_i}{\partial x_j} + \frac{\partial u_j}{\partial x_j}\right)\frac{\partial u_i}{\partial x_j} \quad (6)$$

$C_1 = \max\left[0.43\frac{\mu_t}{\mu_t+5}\right]$, C_2=1.0, σ_k=1.0, σ_ε=1.2,

$$\mu_t = \rho C_\mu \frac{k^2}{\varepsilon} \quad (7)$$

The realizable k-ε turbulence model was adopted in this study which have been validated in our previous works (Liang *et al.* 2019; Xie *et al.* 2018a).

3. EXPERIMENTAL PART

3.1 Experimental Setup

An experimental rig was designed and fabricated to cover the tests under the impact of a dimpled tube for heat transfer improvement and pressure drop in a shell and heat exchanger tube. The following components form the experimental test rig's central part: the external pipe's internal diameter (72mm), external diameter (76mm), and length (l= 1200 mm) are made from stainless steel, while the inner pipe (dimples tube) made from copper with internal diameter (26.2 mm), external diameter (28 mm), and length (l= 1350 mm) where hot water flows within the dimple tube with temperature of 60 C° and cold water flows through the exterior pipe with temperature of 27 C°. A schematic heat exchanger system of shell and tube utilized in the experiment is seen in Figure 3, and the experimental set-up of heat exchanger system is seen in Figure 4. Specific details of the test tube's design are described in table 1. The dimpled tube is designed in a staggered array with pitch ratio x/d=8, with an angle of 60 at 6 mm diameter, as seen in Figure 5; a CNC machine manufactured the tube in the centre of training and workshops at the University of Technology. Also, for the flow measurement, two rotameters (acrylic, 2-18 lpm) for hot water and (acrylic, 0 -35 lpm) for cold water are utilized for inner and outer tubes for enhanced over-discharge control. Two pumps (centrifugal self-primed pump, 3-35 lpm, closed impeller) to feed geyser and (centrifugal self-primed pump, 3-35 lpm, closed impeller) are utilized to create the flow of hot water, while another one pump is needed to create the flow of cold water. Four digital thermometers at each inlet and outlet of each tube have a digital thermometer (C100fk07-m*an, range 0 ºC to 1300ºC) attached to it for monitoring temperature. These thermometers are connected to the temperature indicator. Water manometers of range (10 -1000 pa) were used to measure the pressure difference between hot water and the pressure drop through test tubes.

Table 1 Specifications of dimpled tubes

Dimpled arrangement	Distribution Angle	Diameter D (mm)	Pitch ratio X/D	Dimples spacing X (mm)
Inline	60º	6	8	48
Staggered	60º and 90º	4 and 6	8	48

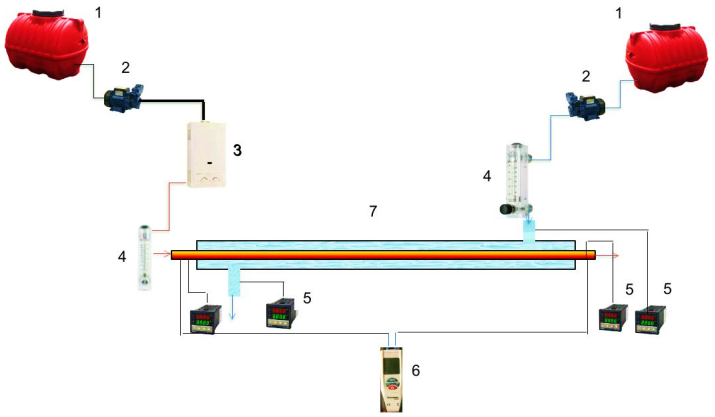

Fig. 3 Schematic diagram of heat exchanger setup:
1- Tank, 2-Pumps, 3-Gas Geyser, 4- Rotameter, 5- Digital Thermocouples, 6- four Manometers, 7- Test Section.

Fig. 4 Experimental set-up of test rig

3.2 Experimental procedure

The experimental steps were described in this section for each test. The experiments were performed on smooth and staggered dimpled tubes with four Reynolds number values of (5000, 10,000, 15,000, and 20,000). The procedures that have been executed during each test are as follows:

- Start the water supply. Adjust the water supply on the hot and cold sides. All connections are inspected to ensure that there is no water leakage.

Global Digital Central
ISSN: 2151-8629

- Cold water is pumped from the cold water tank at 27 degrees to the outer tube
- Switch 'ON' the geyser. The temperature of the water will start rising to until being steady at 60° pumping into the inner copper tube with different mass flow rates
- After temperatures become steady, note down the readings and fill up the observation table.
- Recording the pressure difference between the entry and exit of the copper tube using a pressure gauge
- Making practical calculations according to the recorded readings

3.3 Data Analysis

The averaged Nusselt number Nu_i and thermal performance factor (TPF) are determined based on the test tube's inner diameter. The amount of hot water heat, Q_h, can be calculated by:

$$Q_h = \dot{m}_h CP_h(T_{hi} - T_{ho}) \quad ((6)$$

Where $\dot{m}_h$ is the hot water mass flow rate; T_{hi} and T_{ho} are the inlet and outlet hot water temperatures

$$LMTD = \frac{\Delta T_1 - \Delta T_2}{\ln\left(\Delta T_1 / \Delta T_2\right)} \quad ((7)$$

for the counter-current flow.

$$\Delta T_1 = T_{h,i} - T_{c,o} \; and \; \Delta T_2 \; T_{h,o} - T_{c,i} \quad ((8)$$

To find Nu_i

$$\mathrm{Nu_i} = \frac{\mathrm{h_i\, D_h}}{\mathrm{K}} \quad ((9)$$

Based on the water's characteristics at the area's mean bulk fluid temperature, the fluid's local thermal conductivity (k) is computed. Where

$$D_h = \frac{4A_c}{P} \quad ((10)$$

$D_h = d_i$

To find h_i

$$Q_h = U_i\, A_i\, LMTD \quad (11)$$

Where U_i *Inside overall heat transfer coefficient*

$$A_i = \pi\, d_i L \quad ((12)$$

Where d_i inside diameter of dimple tube

The U_i is determined (by neglecting of the thermal resistance in the copper tube wall) using

$$U_i = \frac{1}{1/h_i} \qquad \therefore \; h_i = U_i \quad ((13)$$

Efficacy of heat transfer enhancement methods can be evaluated using the (TPF), a ratio of changes in heat transfer rate to change in friction factor.

$$TPF = \frac{Nu/Nu_\circ}{(f/f_\circ)^{\frac{1}{8}}} \quad (\quad ($$

Where $f_\circ$ from correlation Petukhov

$$f_\circ = (0.790\; In\; Re_D - 1.64)^{-2} \quad ((15)$$

and f

$$f = \frac{2\Delta P_h d_i}{\rho\, L\, u^2} \quad ((16)$$

$$u = \frac{\dot{m}}{\frac{\pi}{4} d_i^2 \rho} \quad ((17)$$

3.4 Grid Independency

In order to choose a suitable grid accuracy, a grid independence analysis is first achieved, then increasing the mesh's accuracy and recording the results, and continuing to increase the mesh's accuracy until the value of the results remains constant, with the accuracy of the mesh in which the value of the results remains constant being used in the solutions. This test was conducted for three configurations of dimples tubes (smooth tube, dimples tube with d= 6 line 60, stagger 60 at Reynolds number (5,000). According to Figure 5, the average nusselt number remains constant (2,489,956) elements, so this number of cells will be used to solve problems.

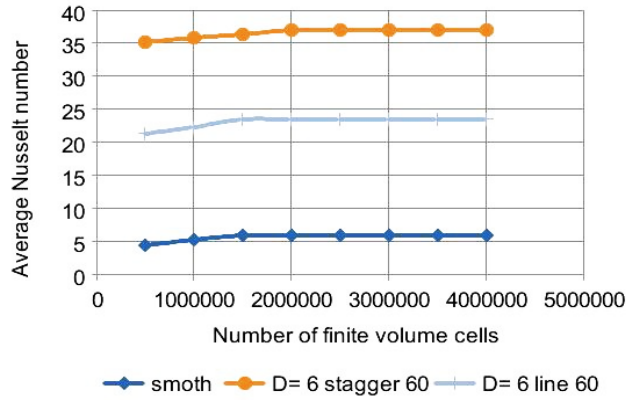

Fig. 5 Average Nusselt number versus number of the finite volume cells for three different types of tubes

4. VALIDATION OF NUMERICAL WORK

Validation work is carried out next to verify the current numerical simulation and compare it with the numerical and experimental performed by thianpong et al. (2009). Figure 6 show deviation of nusselt number ranges from 24 to 45% for numerical result compared with the numerical result by thianpong et al. (2009). This deviation was caused by assuming the constant of fluid properties. The excellent agreement between simulation and experimental results confirms the validity of the physical model used in this study.

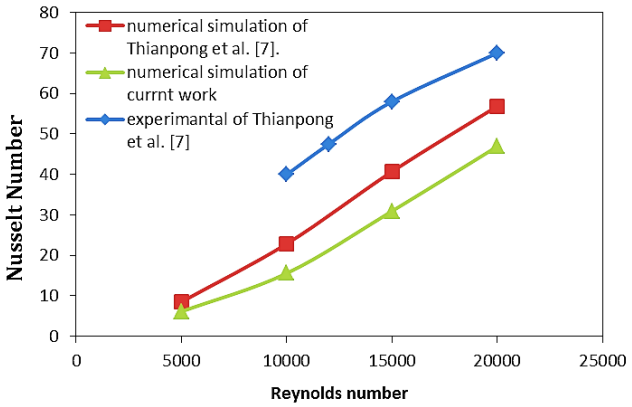

Fig. 6 Comparison simulation results of smooth tube for Nusselt number.

5. RESULTS AND DISCUSSION

This section discusses a number of factors, including the results of numerical research because of the distribution of the dimples into performance and a comparison of experimental and numerical results for the dimple tube. The dimpled tube's thermal performance factor (TPF) is presented.

5.1 Effect of Dimples Arrangement

Numerical analysis is performed on two types of dimpled tubes (Inline and staggered dimpled arrays) with a pitch of X/d=8 at an angle of 60 and a 6 mm diameter, as seen in Table 1.

Figure 7 demonstrates that the staggered array's heat transfer is 50% greater than the inline array's. This is because the staggered array's tubes have increased the turbulence's strength and created strong vortices. It is obvious that similarly to the conventional turbulent flow in a tube, the Nusselts number increase as the Reynolds number increases. A comparison of pressure drop value with several different Reynold numbers is illustrated in Figure 8. It is clear, that the value of pressure drop for staggered array tubes is higher than the value of inline array tubes and then higher than the smooth tubes. Figure 9 shows the numerical results thermal of (TPF) for the dimpled tube array with staggered and inline arrangements. There is a significant increase in heat transfer area in the staggered arrangement of dimple tubes, which increases the thermal performance factor. Tubes arranged in a line had an enhancement ratio that ranged from 1.67 to 5.22, while dimple tubes in staggered arrangement had an enhancement ratio that ranged from 4.91 to 8.633 for a range of Reynolds values (5000-20,000). All additional simulations in this inquiry were conducted using the staggered setup solely after these results were considered.

Figure 10(a) to (c) show the temperature contours for smooth and dimpled tube (in-lined and staggered). Dimples and regular surfaces are two types of heat transfer surfaces in the tube. The staggered tube has a faster heat transfer rate than the inline tube, and the dimpled portions of the tube appear to be where the most heat is transferred. The effect of flow and reattachment in these places of intense turbulence causes high heat transfer on the surfaces of the dimples and the surface in the flow direction. Figure 11 (a) to (c) Display the pressure distribution along the smooth and dimpled tube (in-lined and staggered). As the water flows through the dimple tube, its pressure falls steadily from the tube's highest point to its lowest point. The staggered loses pressure more quickly than the inline, as observed. The boundary layer's development interruption and increased heat transfer turbulence are caused (Promvonge 2008 and Bergles 2002).

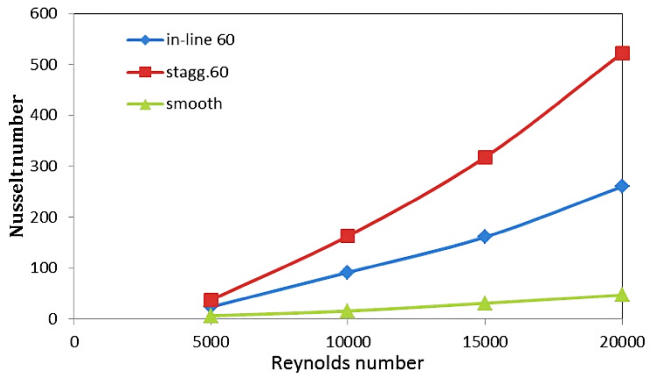

Fig. 7 Effect of Dimples Arrangement.

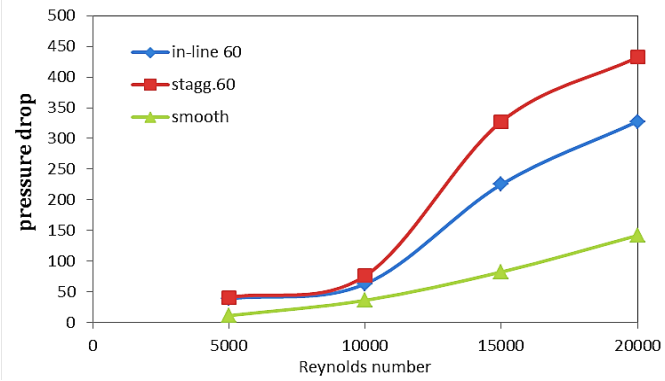

Fig. 8 Effect of Dimples Arrangement on pressure drop.

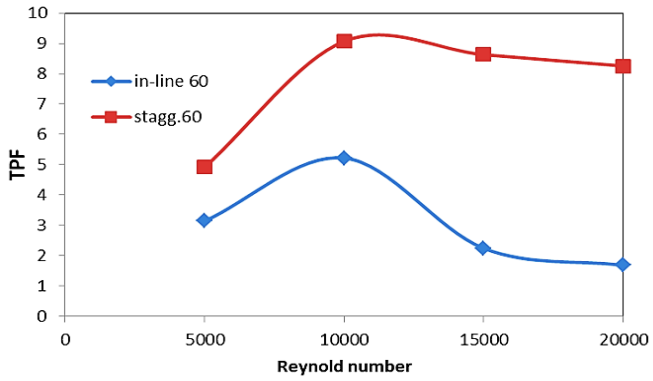

Fig. 9 Thermal Performance Factor (TPF).

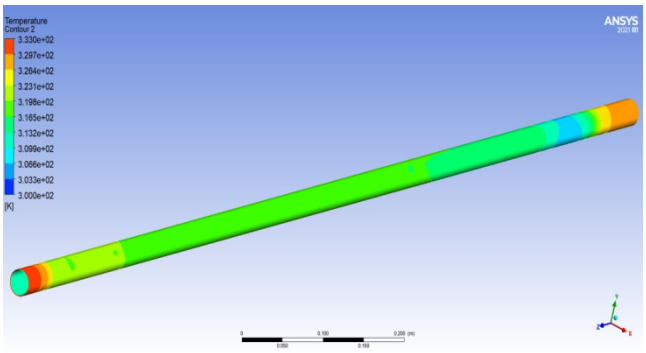

(a) smooth tube

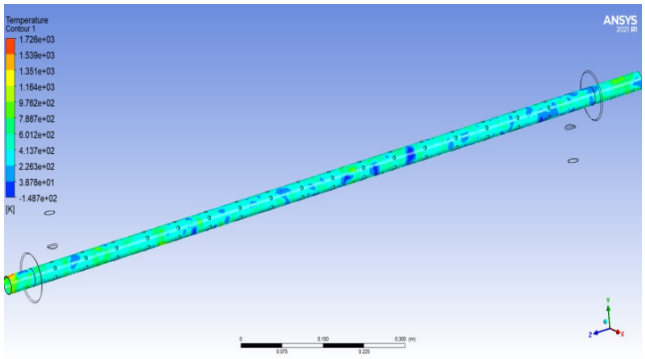

(b) inline dimple tube

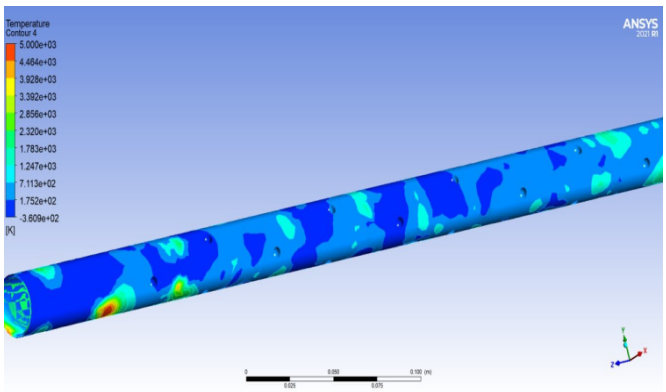

(c) staggered dimple tube

Fig. 10 Temperature contours of (smooth tube, inline dimple tube, and staggered dimple tube).

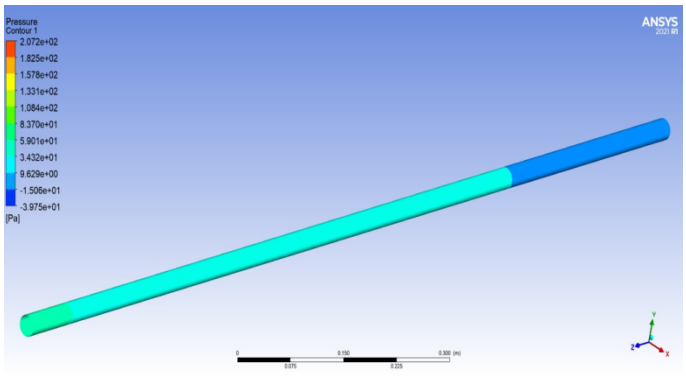

(a) smooth tube

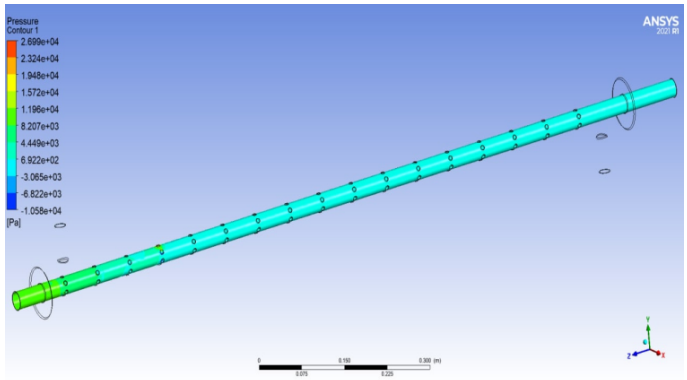

(b) inline dimple tube

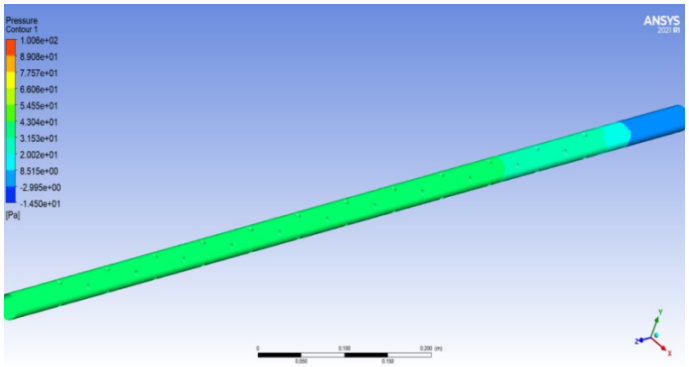

(c) staggered dimple tube

Fig. 11 pressure contours of (smooth tube, inline dimple tube, staggered dimple tube).

5.2 Effects of the Angle Distribution

In figurers12 and 13, the temperature and pressure are shown at different dimpled angles. Additionally, when the dimpled angle decreases, so does the temperature. Increasing the number of dimples on a surface increases the flow impingement and reattachment rate, which improves heat transmission. This phenomenon is primarily owing to this increased rate of flow. Nusselt number and pressure drop are shown in Figure 13 at various angles. The 60° angle provides the best heat transfer performance, followed by the 90° angle. Figure 13c presents the PTF for two angles. Dimpled tubes at 60° had better performance than those at 90°; however, this advantage diminishes as Re increases beyond 10,000. That happens because the thermal-hydraulic performance dominates the heat transfer enhancement.

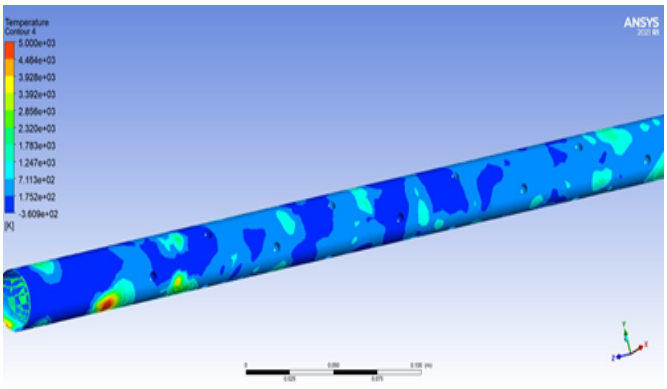

(a)

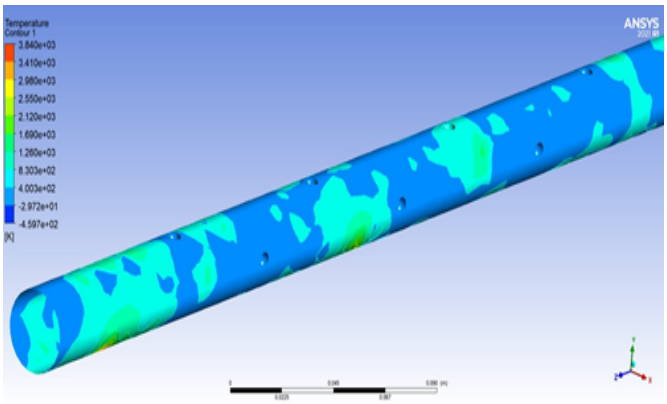

(b)

Fig. 12 Effect of a dimpled angles on temperature distribution at D=6, P=8, and Re= 5,000 (a) angle= 60°, (b) angles= 90º.

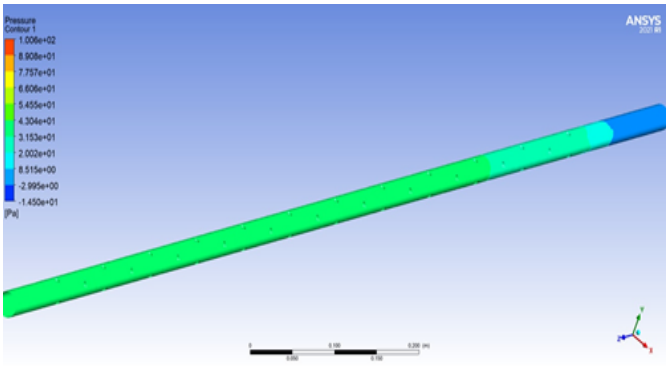

(a)

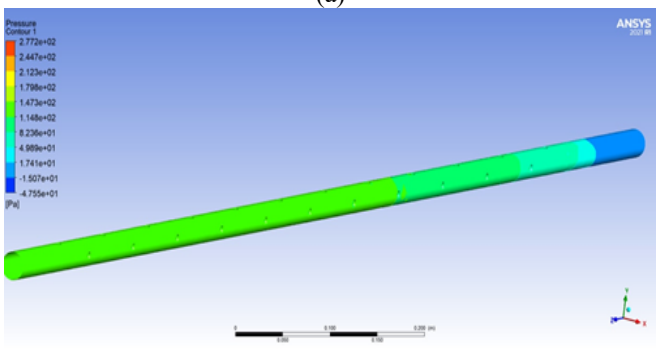

(b)

Fig. 13 Effect of a dimpled angles on pressure distribution at D=6, P=8, and Re= 5,000 (a) angle= 60°,(b) angles= 90º.

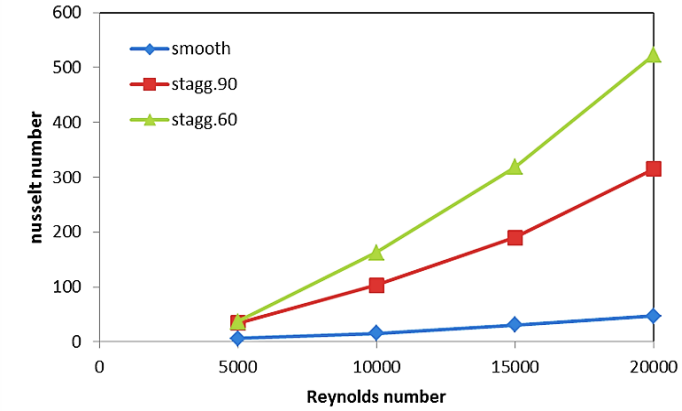

(a)

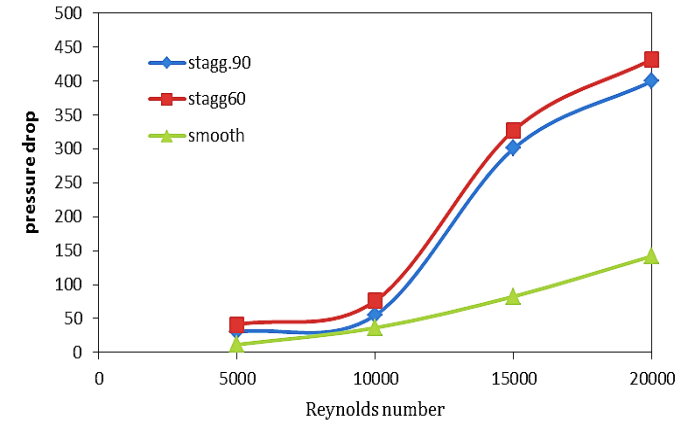

(b)

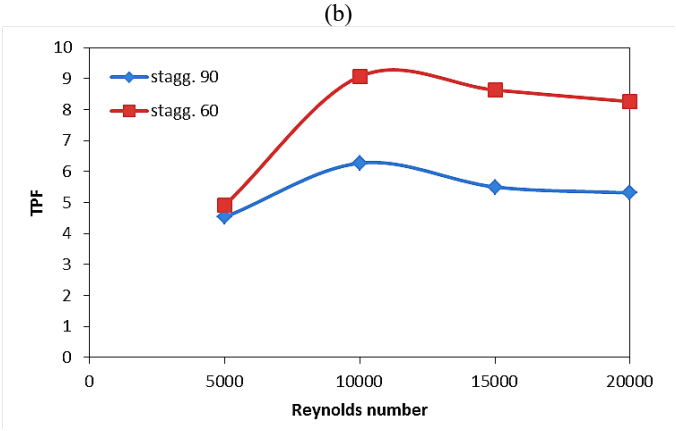

(c)

Fig. 14 Effect of a different dimpled angles on (a) Nusselt number, (b) pressure drop, and (c) TPF.

5.3 Effect of Dimples Diameter

Figures 15 and 16 depict two different dimple diameters. The pressure and temperature rise significantly with the diameter of the dimples. Fig. 17(a) shows Nusselt numbers for various dimple diameters on average. The Nusselt number grows as the Reynolds number increases. D = 6 mm yields the most significant Nusselt number compared to D = 4 mm. This is due to the increased turbulence strength caused by the dimpled tube's enormous diameter creating many vortices. Fig. 17(c) shows the TPF. On the other hand, a PTF of 6mm is more significant than a PTF of 4mm, as can be seen in the image, where the TPF increases as the diameter of the dimples decreases.

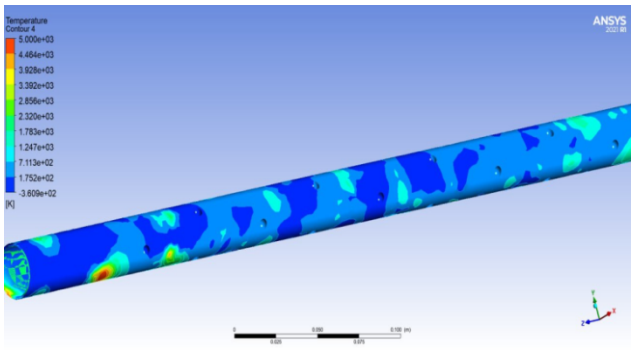

(a)

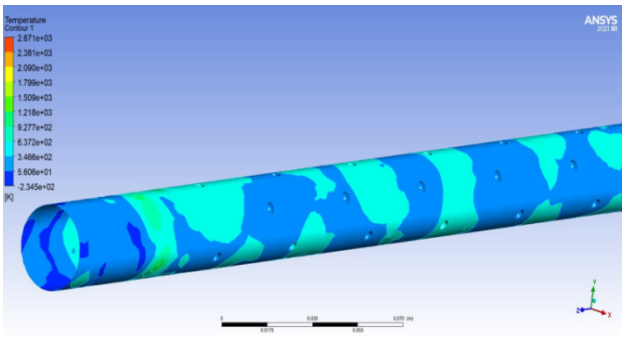

(b)

Fig. 15 Effect of a dimpled diameter on temperature distribution at staggered, angle= 60°, and Re= 5,000 (a) D=6, (b) D=4.

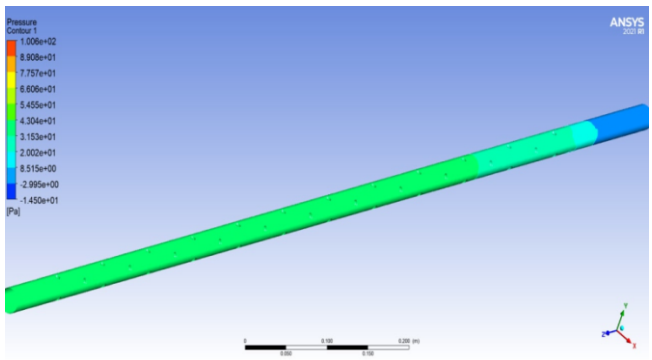

(a)

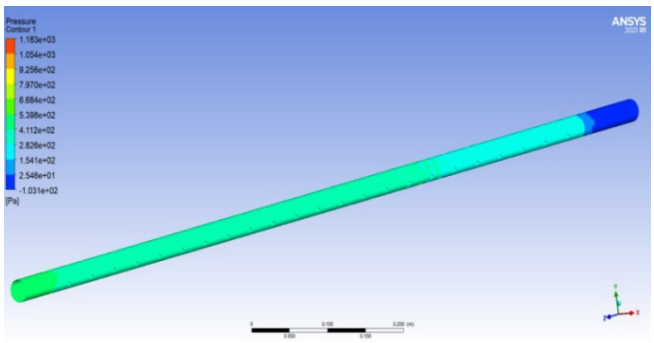

(b)

Fig. 16 Effect of a dimpled diameter on pressure distribution at staggered, angle= 60°, and Re= 5,000, (a) D=6, (b) D=4.

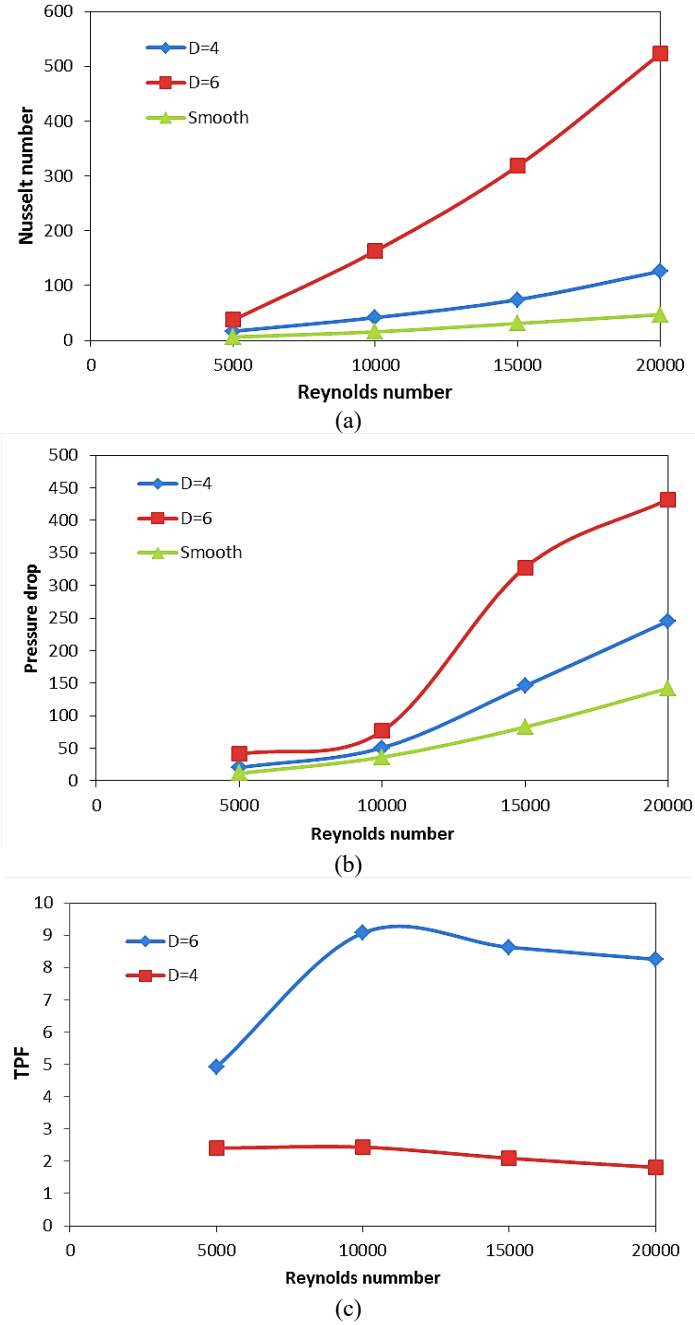

Fig. 17 Effect of a different dimpled diameter ratio on (a) Nusselt number, (b) pressure drop, and (c) TPF.

5.4 Compression Between Dimpled and Plain Tubes

Figure 18 shows Experimental outcomes of (Nu) characteristics in dimpled tubes. The results indicate that the Nusselt number increased with the Reynolds number for conventional turbulent tube flow. The Nusselt number of a dimpled tube is 7.55 to 11.2 times higher than that of a regular tube, based on the Reynolds number (Re). This type of turbulent flow shows a more significant increase in the Nusselt number due to a greater decrease in the thickness of the boundary layer and an increase in heat transfer. The turbulence results from the difference in the flow and direction of the fluid, which may sometimes intersect or even move in the opposite direction, as these swirl flows begin to move the flow using the increased energy, which leads to an increase in heat transfer. Figure 19 illustrates the value of the pressure drop for a variety of various Reynold values. It is abundantly evident that the pressure drop value for dimpled tubes with staggered array tubes is significantly greater than the value of the smooth tubes.

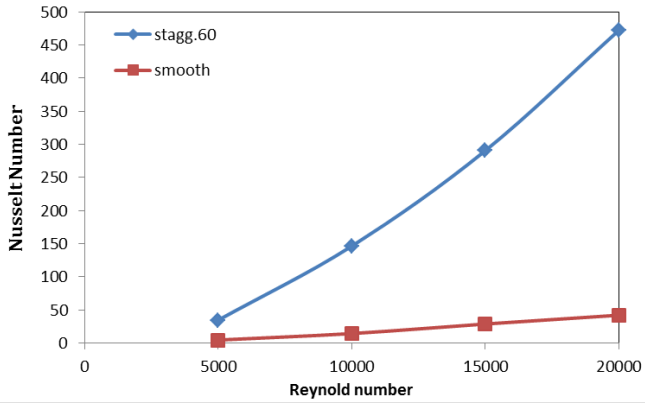

Fig. 18 Compression between plain and dimpled tube.

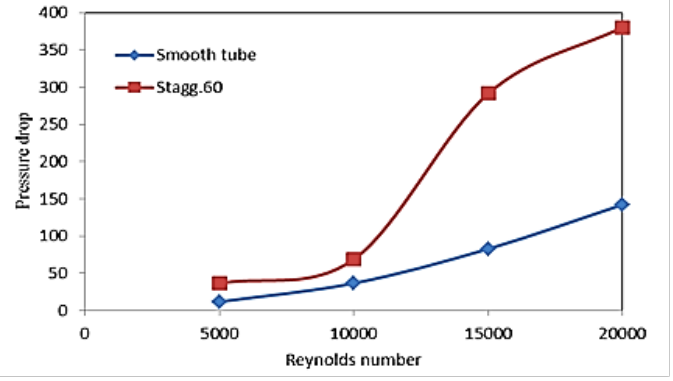

Fig. 19 Compression between plain and dimpled tube.

5.5 Comparisons of Experimental and Numerical Present Results

Figure 20, 21and 22 demonstrate the comparison of heat transfer data for the dimpled tube with staggered layouts from numerical and experimental methods. The experimental and numerical results show good agreement. Good agreement can be seen between the experimental and numerical results, 7.5–10.6 percent greater for numerical for low and high Reynolds numbers, respectively.

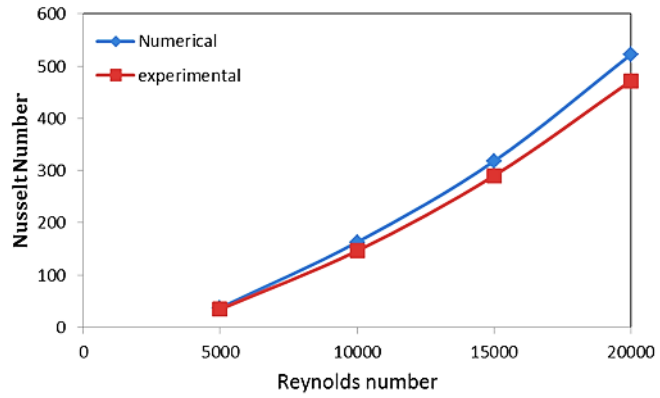

Fig. 20 Comparison of experimental with numerical results for inner staggered tube (60º) for Nusselt number.

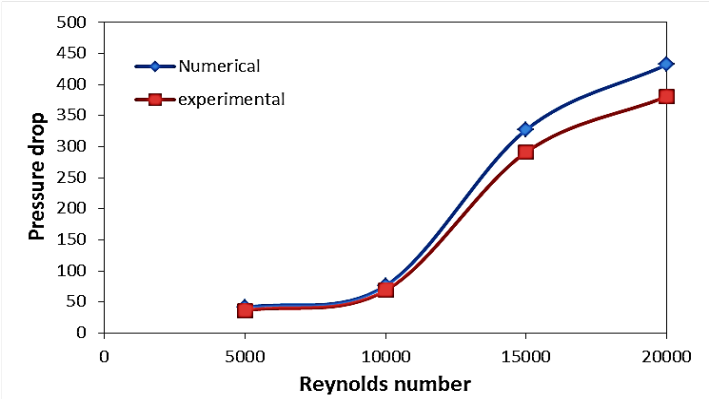

Fig. 21 Comparison of experimental with numerical results for inner staggered tube (60º), (pressure drop).

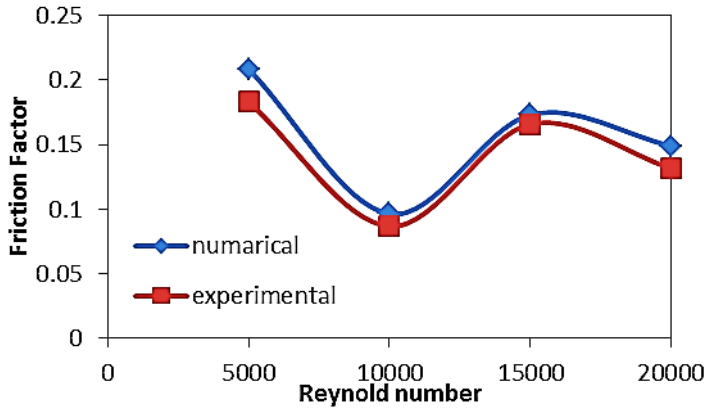

Fig. 22 Comparison of experimental with numerical results for inner staggered tube (60º), (friction factor)..

5. CONCLUSIONS

This paper numerically and experimentally investigates the heat performance and flow properties of dimpled inner tube for double pipe heat exchanger, the main conclusion are summarized as follows :

- Numerical analysis is performed on two types of dimpled tubes (Inlined and staggered dimpled arrays). It's observed that the Nusselt number of the staggered array higher than the inline array.
- The dimpled tube staggered arrangement showed an enhancement about 50% than that an in-lined dimpled arrangement for double pipe heat exchanger.
- The influence of two dimple dimensions D= 4,6 on the heat transfer process is investigated. Using D = 6 mm instead of D = 4 mm, more heat is transferred because the bigger diameter causes more flow and dissipation to be obstructed, and therefore more heat is dissipated.
- The effect of dimpled angles, pitch, and diameter make a significant difference in heat and transfer characteristics. The staggered arrangement, angle with 60°, P = 8 mm, and D=8, shows the best result of Nusselt number drop pressure the maximum TPF performance
- Nusselt numbers increase as Reynolds numbers increase due to increased turbulent flow degrades the flow path as the Reynolds number rises, leading to an increase in the Nusselt number, which results in a more turbulent flow.
- Thermal performance factor in the dimple tube with staggered arrangement was higher than tube with line arrangement about 50 %
- Good agreement is obtained between the experimental and the numerical results

ACKNOWLEDGEMENTS

Authors would like to thank Mustansiriyah university (www.uomustansiriyah.iq) Baghdad, Iraq for its support in present study.

REFERENCES

Ali, A., Wahlquist, S., Yoon, S.J. and Sabharwall, P., 2022, "Laminar Flow Heat Transfer In Helical Oval-Twisted Tube For Heat Exchanger Applications," *Frontiers in Heat and Mass Transfer (FHMT)*, 18, p.8. http://dx.doi.10.5098/hmt.18.35.

Aroonrat, K. and Wongwises, S., 2017, "Experimental study on two-phase condensation heat transfer and pressure drop of R-134a flowing in a dimpled tube," *International Journal of Heat and Mass Transfer*, 106, 437-448.

http://dx.doi.org/10.1016/j.ijheatmasstransfer.2016.08.046

Bejan A., A. D. 2003, *Heat Transfer Handbook*, John Wiley & Sons, Inc., Hoboken, New Jersey.

Bergles, A.E., 2002, "ExHFT for fourth generation heat transfer technology," *Experimental Thermal and Fluid Science*, 26(2-4), 335-344. http://dx.doi.org/10.1016/S0894-1777(02)00145-0

Chen, J., Müller-Steinhagen, H. and Duffy, G.G., 2001, "Heat transfer enhancement in dimpled tubes," *Applied thermal engineering*, 21(5), 535-547. http://dx.doi.org/10.1016/S1359-4311(00)00067-3

Datt, R., Kumar, A., Bhist, M.S., Kothiyal, A.D. and Maithani, R., 2019, "Hydrodynamic and thermal performance twisted tape insert provided in heat exchanger tubes: a review," *Frontiers in Heat and Mass Transfer (FHMT)*, 12, p.26. http://dx.doi.10.5098/hmt.12.26.

Davidson, L. 2009, An Introduction to Turbulence Models, Department of Thermo and Fluid Dynamics, Chalmers University of Technology, Sweden. http://dx.doi.org/10.1007/978-94-011-4515-2_4.

Fan, Q. and Yin, X., 2008, "3-D numerical study on the effect of geometrical parameters on thermal behavior of dimple jacket in thin-film evaporator," *Applied thermal engineering*, 28(14-15), 1875-1881. http://dx.doi.org/10.1016/j.applthermaleng.2007.11.024

Jalghaf, H.K. and Hatem, F.F., 2017, "Experimental and Numerical Investigation of Slot Dimple Tube on the Heat Exchanger Performance," *Kufa Journal of Engineering*, 8(3), 1-20.

Kumar, P., Kumar, A., Chamoli, S. and Kumar, M., 2016, "Experimental investigation of heat transfer enhancement and fluid flow characteristics in a protruded surface heat exchanger tube," *Experimental Thermal and Fluid Science*, 71, 42-51. http://dx.doi.org/10.1016/j.expthermflusci.2015.10.014

Li, M., Khan, T.S., Al Hajri, E. and Ayub, Z.H., 2016, "Geometric optimization for thermal–hydraulic performance of dimpled enhanced tubes for single phase flow," *Applied thermal engineering*, 103, 639-650. http://dx.doi.org/10.1016/j.applthermaleng.2016.04.141

Li, M., Khan, T.S., Al-Hajri, E. and Ayub, Z.H., 2016, "Single phase heat transfer and pressure drop analysis of a dimpled enhanced tube," *Applied Thermal Engineering*, 101, 38-46. http://dx.doi.org/10.1016/j.applthermaleng.2016.03.042

Liang, Z., Xie, S., Zhang, J., Zhang, L., Wang, Y. and Ding, H., 2019, "Numerical investigation on plastic forming for heat transfer tube consisting of both dimples and protrusions," *The International Journal of Advanced Manufacturing Technology*, 102(1), 775-790. https://link.springer.com/article/10.1007%2Fs00170-018-3057-8

Liang, Z., Xie, S., Zhang, L., Zhang, J., Wang, Y. and Yin, Y., 2017, "Influence of geometric parameters on the thermal hydraulic performance of an ellipsoidal protruded enhanced tube," *Numerical Heat Transfer, Part A: Applications*, 72(2), 153-170. http://dx.doi.org/10.1080/10407782.2017.1359000

Promvonge, P., 2008, "Thermal augmentation in circular tube with twisted tape and wire coil turbulators," *Energy Conversion and Management*, 49(11), 2949-2955. http://doi.org/10.1016/j.enconman.2008.06.022 .

Shafaee, M., Mashouf, H., A. Sarmadian, Mohseni, S. G. (2016): Evaporation heat transfer and pressure drop characteristics of R-600a in horizontal smooth and helically dimpled tubes, *Applied Thermal Engineering,* Vol. 107 pp. 28-36. http://dx.doi.org/10.1016/j.applthermaleng.2016.06.148

Solanki, A.K. and Kumar, R., 2018, "Condensation of R-134a inside dimpled helically coiled tube-in-shell type heat exchanger," *Applied Thermal Engineering*, 129, 535-548. http://dx.doi.org/10.1016/j.applthermaleng.2017.10.026

Thianpong, C., Eiamsa-Ard, P., Wongcharee, K. and Eiamsa-Ard, S., 2009, "Compound heat transfer enhancement of a dimpled tube with a twisted tape swirl generator," International communications in heat and mass transfer, 36(7), 698-704. http://dx.doi.org/10.1016/j.icheatmasstransfer.2009.03.026

Vignesh, S., Moorthy, V.S. and Nallakumarasamy, G., 2017, "Experimental and CFD analysis of concentric dimple tube heat exchanger," *Int. J. Emerg. Technol. Eng. Res.(IJETER)*, 5(7), 18-26.

Wang, Y., He, Y.L., Lei, Y.G. and Zhang, J., 2010, "Heat transfer and hydrodynamics analysis of a novel dimpled tube," *Experimental thermal and fluid science*, 34(8), 1273-1281. http://dx.doi.org/10.1016/j.expthermflusci.2010.05.008

Wang, Y., He, Y.L., Li, R. and Lei, Y.G., 2009, "Heat transfer and friction characteristics for turbulent flow of dimpled tubes," Chemical Engineering & Technology: Industrial Chemistry-Plant Equipment-Process Engineering-Biotechnology, 32(6), 956-963. http://dx.doi.org/10.1002/ceat.200800660

Xie, G., Liu, J., Zhang, W., Lorenzini, G. and Biserni, C., 2014, "Numerical prediction of flow structure and heat transfer in square channels with dimples combined with secondary half-size dimples/protrusions," *Numerical Heat Transfer, Part A: Applications*, 65(4), 327-356..

Xie, S., Liang, Z., Zhang, J., Zhang, L., Wang, Y. and Ding, H., 2019, "Numerical investigation on flow and heat transfer in dimpled tube with teardrop dimples," *International journal of heat and mass transfer*, 131, 713-723. http://dx.doi.org/10.1016/j.ijheatmasstransfer.2018.11.112

Xie, S., Liang, Z., Zhang, L. and Wang, Y., 2018b, "A numerical study on heat transfer enhancement and flow structure in enhanced tube with cross ellipsoidal dimples," *International Journal of heat and mass transfer*, 125, 434-444. http://dx.doi.org/10.1016/j.ijheatmasstransfer.2018.04.106

Xie, S., Liang, Z., Zhang, L., Wang, Y., Ding, H. and Zhang, J., 2018a, "Numerical investigation on heat transfer performance and flow characteristics in enhanced tube with dimples and protrusions," *International Journal of Heat and Mass Transfer*, 122, 602-613.http://dx.doi.org/10.1016/j.ijheatmasstransfer.2018.01.106

Zheng, L., Zhang, D., Xie, Y. and Xie, G., 2016, "Thermal performance of dimpled/protruded circular and annular microchannel tube heat sink," Journal of the Taiwan Institute of Chemical Engineers, 60, 342-351. http://dx.doi.org/10.1016/j.jtice.2015.10.026